Macromolecules

ARTICLE

pubs.acs.org/Macromolecules

Rapid Assembly of Nanolines with Precisely Controlled Spacing from Binary Blends of Block Copolymers

Xiaojiang Zhang,[†,‡] Jeffrey N. Murphy,[†,‡] Nathanael L. Y. Wu,[†,§] Kenneth D. Harris,[*,†] and Jillian M. Buriak[*,†,‡]

[†]National Institute for Nanotechnology (NINT), National Research Council, 11421 Saskatchewan Drive, Edmonton, Alberta T6G 2M9, Canada

[‡]Department of Chemistry, University of Alberta, Edmonton, Alberta T6G 2G2, Canada

[§]Department of Electrical and Computer Engineering, University of Alberta, Edmonton, Alberta T6G 2G8, Canada

Supporting Information

ABSTRACT: Thin films cast from binary blends of structurally homologous polystyrene-*block*-poly(2-vinylpyridine) polymers were used to obtain horizontal arrays of linear nanostructures which were visualized by metallizing the poly(2-vinylpyridine) blocks with a tetrachloroplatinate salt. By varying the blend compositions of the homologous block copolymers, fine control over the periodicity of lines was realized from ∼25 to 55 nm using a set of just 4 block copolymers. For neat block copolymers whose equilibrium structures are not horizontal cylinders, blending enabled cylindrical structures to form. The ordering in various films was studied by measurements of defect density, and it was found that in many cases blended films produced patterns of lower defect density than patterns formed from single component block copolymers. Annealing of the polymer films was carried out using a solvothermal microwave annealing technique able to rapidly produce few-defect films. Here the technique is adapted to use a household microwave oven (cost < $100) to rapidly induce self-assembly in under 2 min, enabling broad accessibility.

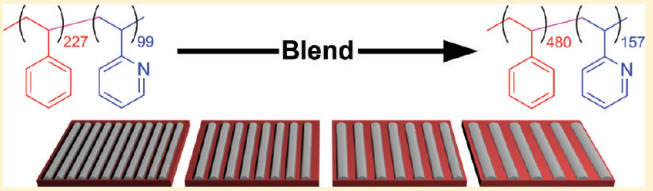

INTRODUCTION

The International Technology Roadmap for Semiconductors (ITRS-2009) describes the self-assembly of block copolymers (BCPs) as an emerging, innovative technology that provides new strategies to generate high-resolution patterns with nanoscale precision.[1] The basic principle underpinning the technology is the short-range phase separation of chemically distinct blocks in a polymer film, and with the selection of appropriate conditions, regular patterns of phase separated structures form spontaneously over large areas. The applications are expected to include nanolithography and nanostructure templating,[2−14] but to truly implement the technology, some key research challenges must be overcome: reducing the time required for pattern formation, improving the alignment, reducing defect density, and precisely tuning the feature spacing.[1,3,15,16]

While feature size and spacing in block copolymers can be controlled synthetically by varying the lengths and proportions of each block,[17,18] this can be laborious and difficult to precisely reproduce, resulting in coarse approximations of the desired domain sizes. Researchers at present must, however, either undertake these synthetic activities or adapt their goals to accommodate the limited selection of readily available commercial materials. Thus, means of fine-tuning BCP patterns without resorting to polymer synthesis would be useful. Tuning of the feature spacing, using a nonsynthetic approach, has previously been effected for lamellar BCP bulk films by applying electric fields, leading to contraction of the interlamellar spacing of up to 6%.[19] Another approach that has previously been undertaken involved blending BCPs with homopolymers to make binary blends,[20−23] which permits control over the domain size and spacing in vertically aligned cylinders and lamellae.[24−28] The addition of large amounts of homopolymer (∼30% by volume fraction), however, results in nonuniform structures and ultimately the loss of phase segregation;[24] this can be overcome, in part, using chemically prepatterned substrates.[29] Past research efforts have also examined the behavior of blends of BCPs in bulk,[30] showing lamellar structures with interlayer spacings that, for binary BCP blends, exhibit a linear dependence on the molar proportions of each polymer.[31] Other work has investigated the localization of chains within binary blends[32] and control of morphology via blending.[33] Recently blending of BCPs has been applied to creation of tunable optical filters from BCP blends.[34] Here we examine thin films cast from two-component blends of homologous BCPs to form horizontally aligned cylinders. Blending enables fine control over feature spacing in nanoscale patterns templated from the cylindrical domains, while using a minimal set of polymers. Aligned, linear BCP patterns with tunable spacings, ranging from 55 to 25 nm, can be obtained in this manner.

Received: September 9, 2011
Revised: October 14, 2011
Published: November 21, 2011

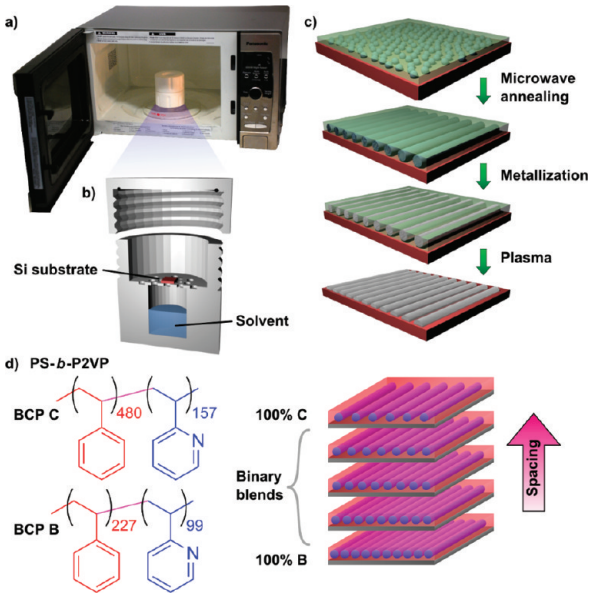

Figure 1. (a) Photograph of a sealed Teflon annealing chamber inside a household microwave oven. (b) Illustration of a cross-section of the loaded annealing chamber. (c) Sequence of steps in a typical experiment: microwave annealing to produce horizontal cylinders, followed by metallization and plasma etching to visualize the patterns. (d) Structures of BCP C and BCP B, which are blended to produce cylinders with intermediate periodicities.

Our previous work took a step toward addressing the issue of long annealing times, demonstrating a microwave-based solvothermal annealing process to accelerate the self-assembly of block copolymer patterns, using a costly, research-grade microwave instrument.[35] Here, we increase the accessibility of the process by using an inexpensive household microwave oven to attain rapid ordering—in under 90 s using an apparatus obtained for less than $100 USD. Furthermore, we have demonstrated that this can be accomplished in a safe and reproducible manner.

EXPERIMENTAL SECTION

Materials and Cleaning Protocols. Chemicals used for wet processing and solvents were obtained from Sigma-Aldrich; PS-*b*-P2VP BCPs were obtained from Polymer Source Inc.; silicon wafers were obtained from University Wafer. Silicon substrates were cut into 1 cm × 1 cm pieces from prime-grade 4-in. Si (100) wafers (10−20 Ω·cm; P-doped with boron; 525 ± 25 μm). The silicon pieces were degreased in an ultrasonic bath of methanol, rinsed in acetone and ethanol, and then dried in a stream of nitrogen gas. Standard piranha and RCA II cleaning procedures[36] were then conducted: first, the silicon pieces were immersed in a piranha solution [3:1, v/v conc. H_2SO_4 (aq) and 30% H_2O_2 (aq)] at 80 °C for 20 min. The silicon pieces were removed from solution, rinsed with water, dried in a nitrogen stream and immersed in an RCA II solution of 38% HCl (aq), 30% H_2O_2 (aq), and Millipore water in a ratio of 1:1:5 at 80 °C for 20 min. The silicon substrates were then removed from the hot solution, rinsed with water, and dried under a nitrogen gas flow.

Blending of Block Copolymers. To prepare the block copolymer thin films, the PS-*b*-P2VP BCPs were weighed, dissolved in neat toluene, and stirred overnight at room temperature to make 1% w/w or 1.5% w/w solutions. Binary blends were prepared by mixing two 1.5% w/w solutions in volume ratios from 1:9 to 9:1 at room temperature and stirring overnight prior to deposition. An aliquot of block copolymer solution (15.0 μL) was then dropped onto the silicon substrate and spin-cast, at 4200 rpm for the 1.5% w/w solutions or at 3800 rpm for the 1% w/w solutions, for 15 s under an argon environment to form a thin film. By fixing both the concentration (w/w) of the BCPs in solution and the spin speed, the thickness of the deposited films was consistently controlled to be ∼42 nm.

Table 1. Table of Commercially Available PS-*b*-P2VP BCPs Used in This Study, Identified in the Text by the Letter Given

BCP	PS (M_n)	P2VP (M_n)	PDI
A	17.0k	9.8k	1.06
B	23.6k	10.4k	1.04
C	50.0k	16.5k	1.09
D	125.0k	58.5k	1.05
E	32.5k	12.0k	1.05
F	44.0k	18.5k	1.05

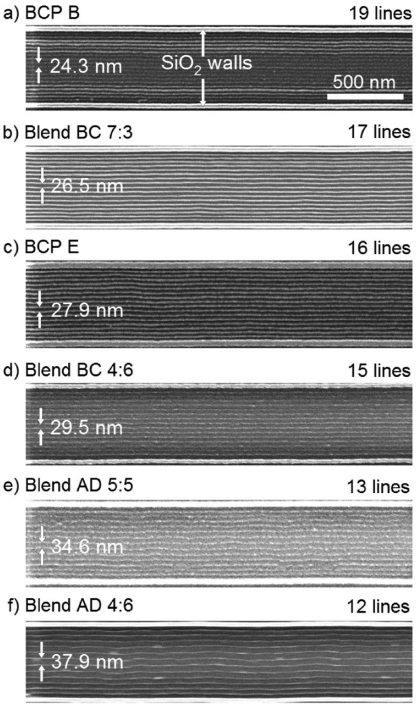

Figure 2. Linear feature spacing control along graphoepitaxially spaced lines 500 nm apart. SEM images of Pt nanostructures with six different spacings, templated by two neat BCPs and four blends: (a) BCP B, (b) blend BC 7:3, (c) BPC C, (d) blend BC 4:6, (e) blend AF 5:5, and (f) blend AD 4:6. In all cases, the microwave annealing time was 80 s.

Microwave Annealing Procedure. Prior to microwave annealing, the BCP-coated silicon substrates were sealed in a custom-made Teflon microwave annealing chamber with 1 mL warm THF in the reservoir. The Teflon chamber was placed on an inverted glass Petri dish (to keep the chamber stationary above the rotary components) in the center of a conventional, household microwave oven (Panasonic Compact Stainless Steel Microwave Oven, NNSD377S) and heated with the maximum power (800 W). The samples were then removed from the Teflon container and cooled in air.

CAUTION! First, given the small amount of microwave absorbing material, annealing times must be limited to prevent overheating and damage to either the annealing chamber or microwave oven. This is particularly important for strongly absorbing substrates. Second, in the

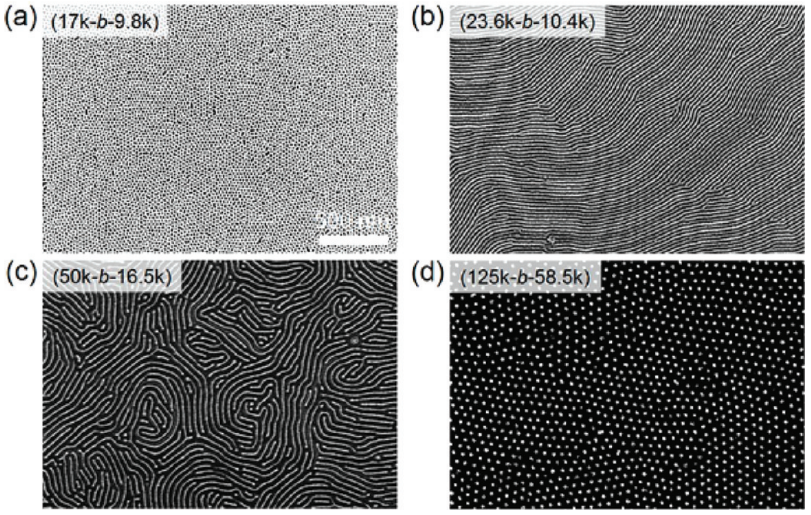

Figure 3. SEM images of Pt nanopatterns templated from neat PS-*b*-P2VP BCPs that were microwave annealed for 60 s: (a) BCP A [PS(17.0k)-*b*-P2VP(9.8k)], (b) BCP B [PS(23.6k)-*b*-P2VP(10.4k)], (c) BCP C [PS(50.0k)-*b*-P2VP(16.5k)], and (d) BCP D [PS(125.0k)-*b*-P2VP(58.5k)].

presence of microwave radiation, electrical arcing and plasma discharge may result from concentrated electric field lines at sharply pointed vertices of silicon substrates or the junction between two substrates, hence substrates with sharp points should be avoided, and multiple substrates must not be placed in close proximity. One incident in our lab—the only one in the course of several hundred experiments and samples—resulted in damage to the annealing chamber when two substrates were in contact during a 3 min anneal. (See Supporting Information for details.) Following these guidelines should prevent such occurrences.

The experimental process for producing thermally annealed controls is described in detail in the Supporting Information.

BCP Visualization by Metallization. The patterns formed by the block copolymers were visualized by metallization with platinum and electron microscopy. The annealed samples were first immersed in an aqueous solution of Na_2PtCl_4 (20 mM) with HCl (1.6%) for 3 h in a glass vial; the protic acid functions to protonate the P2VP blocks, resulting in the swollen P2VP domains rupturing through the PS surface, permitting permeation of the metal salt. The samples were then removed from the solution, rinsed with 18 MΩ·cm water, and dried under a nitrogen gas flow. Oxygen plasma (Harrick Plasma Cleaner/Sterilizer PDC-32G) at 0.12 Torr for 1 min was used to reduce bound $PtCl_4^{2-}$ ions to platinum metal and to etch the polymer matrix.[37,38]

Directed Assembly by Graphoepitaxy. Graphoepitaxy uses topographical features to guide the assembly of BCP structures into highly ordered patterns.[39] In this work, line patterns were written (using the RAITH 150-TWO electron beam lithography system) on substrates with films of resist (Dow Corning XR-1541). A subsequent development step in tetramethylammonium hydroxide (TMAH) produced linear silica topographical features, which control the orientation and position of the cylindrical structures formed by the polymer self-assembly during the microwave anneal.

Image Analysis. SEM images were analyzed using routines developed for ImageJ, and defect densities were determined as in our previous work.[40] The periodicity of the striped patterns was determined using fast Fourier transforms of the images; multiple samples were used for each point.

RESULTS AND DISCUSSION

Microwave Annealing and Blending. The apparatus and processes used for rapid block copolymer self-assembly in the microwave, along with the process used to enhance visualization of the resulting patterns, are briefly outlined in Figure 1. Our previous work showed low defect densities were attained in minutes, and factors such as choice of solvent, annealing time, temperature/power, and substrate resistivity were critical for controlling the BCP self-assembly.[35] Because microwave annealing is a solvothermal process, where both substrate and solvent are heated[41] via microwave irradiation, the optimal silicon substrates were chosen based on a simple measurement of their ability to melt paraffin wax (see Supporting Information). These selected silicon substrates (i.e., 10−20 Ω·cm, p-doped, <100>) were cleaned and spin-coated with polystyrene-*block*-poly(2-vinylpyridine) (PS-*b*-P2VP) solutions to form BCP thin films roughly 42 nm thick, as measured by ellipsometry.

Several commercially available BCPs were investigated both neat and as binary blends. The properties of each BCP are described in Table 1, and blends are denoted with their constituents and volume ratio. For example, blend AB 2:8 refers to PS(17.0k)-*b*-P2VP(9.8k) (A) combined with PS(23.6k)-*b*-P2VP(10.4k) (B) in a 2:8 ratio by mass. As spin-coated, the BCP films formed quasi-ordered hexagonal patterns on the silicon surfaces. These samples were then microwave annealed in a sealed Teflon chamber (photographs in Supporting Information) preloaded with tetrahydrofuran (THF), as shown in Figure 1, parts b and c. A conventional microwave oven with a maximum power of 800 W was employed, providing the energy required to facilitate the organization of linear structures. The annealing chamber was always placed stationary in the center of the microwave oven to limit any effects due to anisotropy in the electromagnetic field (Figure 1a). Finally, the metallization and plasma processes described previously were undertaken (Figure 1c) to make the patterns visible by scanning electron microscopy (SEM).[37,38]

Effect of Blending on Periodicity. A series of neat and blended BCPs was chosen to demonstrate the precise control over spacing (illustrated in Figure 1d) that can be obtained via graphoepitaxially directed self-assembly between parallel silica walls with an 80 s anneal in the microwave. As shown in Figure 2, the number of patterned lines in the 500 nm wide channels could be controlled exactly: 19, 17, 16, 15, 13, and 12 lines are shown

self-assembled within the graphoepitaxial features, using a combination of neat and blended BCPs. As an example, for BCP B, the spacing was adjusted by blending with BCP C to produce defect-free patterns with feature spacings of 24.3, 26.5, and 29.5 nm as shown in Figure 2.

To demonstrate control over the periodicity of the templated patterns, a 60 s microwave anneal procedure was applied to a series of neat BCPs (A, B, C, and D) and block copolymer blends (AC, BC, AD, and BD). The patterns formed by the neat BCPs, A, B, C, and D, are shown in Figure 3. The structures formed by BCPs A and D are noncylindrical, and the cylindrical patterns formed by BCPs B and C incorporate several defects.

SEM images of the Pt nanostructures templated from microwave annealed block copolymer blends together with the corresponding measured feature spacings and defect densities are shown in Figure 4. In general, a roughly linear progression from the natural periodicity of one block copolymer to that of the second block copolymer was observed as the two constituents were blended. This property should allow the assembly of any desired spacing within the dynamic range of the two block copolymers. In contrast to the loss of phase segregation observed in block copolymer blends with large quantities of homopolymers,[24] the PS-*b*-P2VP/PS-*b*-P2VP binary blends provide good control over the linear feature spacing while in all proportions retaining the microphase-separation of the polymer blocks and the long-range cylindrical morphology of the self-assembled block copolymers. Furthermore, these results contribute to the revision of the generally held assumption that block copolymers must possess a low polydispersity index (PDI) in order to form well ordered, microphase-separated structures by self-assembly,[42] as these blends of homologous block copolymers are polydisperse by their very nature, yet form well-ordered structures.[43] PS-*b*-P2VP multicomponent blends have been explored, however these studies were focused on understanding the effects of polydispersity on thermally annealed thick films with lamellar morphology, which needed to be sectioned by an ultramicrotome for structural visualization.[44,45]

Furthermore, BCPs for which horizontal cylinders are not the minimum free energy configuration may be combined with other BCPs to form thin films of cylindrical structures—even in the case where neither BCP naturally forms horizontal cylinders, as demonstrated by blend AD in Figure 4c. In isolation, BCP A forms an array of PS dots in a P2VP matrix (shown in Figure 3a), and BCP D forms an array of P2VP dots in a PS matrix (shown in Figure 3d), yet a horizontal, cylindrical structure is created upon blending in suitable fractions. Investigations of the morphological changes resulting from blending have been investigated,[32,33] however it has not been applied to any significant extent. This may open the door to accessing various block copolymer morphologies in thin films via blending homologous polymers rather than endeavoring to synthesize new BCPs with appropriate block lengths.

To quantify the order and the relative quality of each sample, the defect density is measured relative to a perfectly aligned striped pattern free of dots, junctions, and terminal points. Defects are pairs of such component structures formally described as either dislocations or disclinations.[46] Because of the large number of images, we quantify the number of defects per unit area using a computer-assisted counting algorithm to provide the defect density.[35] It can be observed from the plots of defect density in Figure 4 that for any given pair of BCPs, the defect density minimum is generally observed with one of the

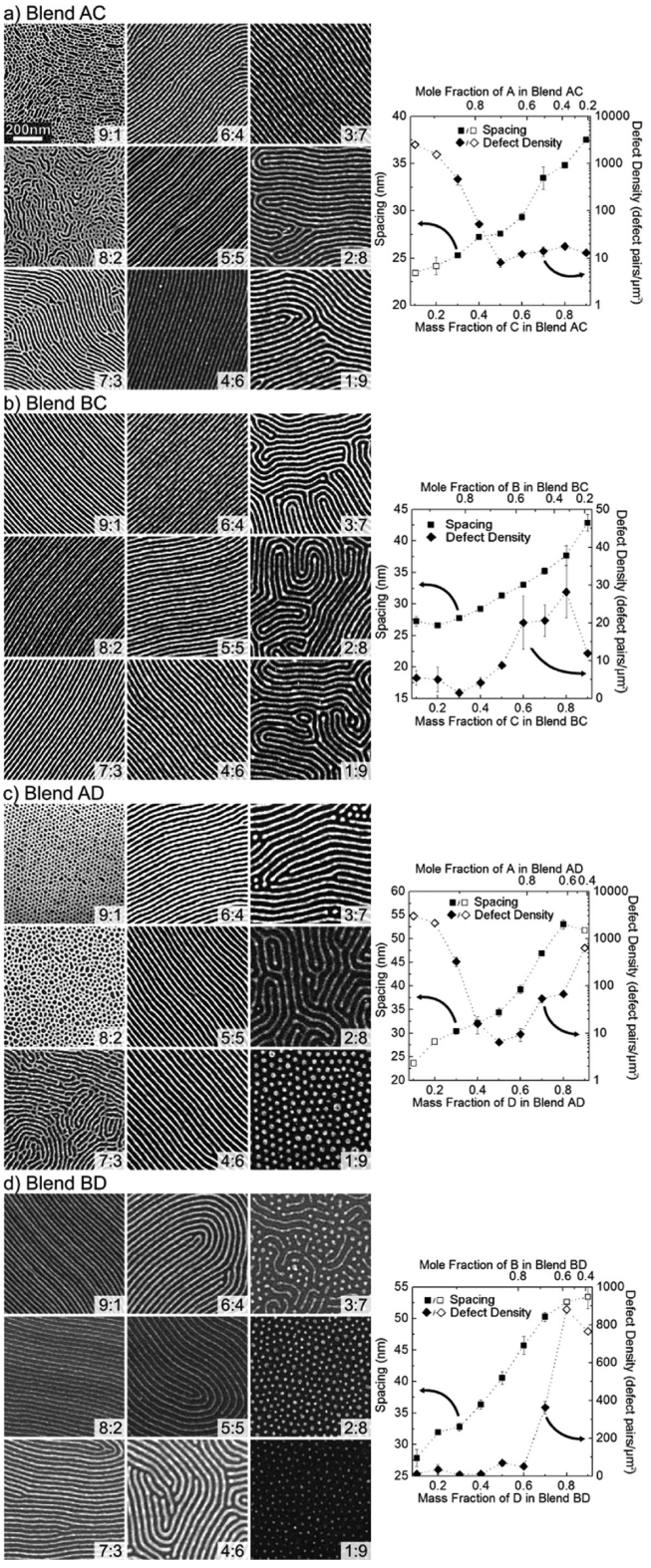

Figure 4. SEM images of Pt nanopatterns templated from PS-*b*-P2VP/PS-*b*-P2VP binary blends that were microwave annealed for 60 s. (a) Blend AC 9:1 to 1:9. (b) Blend BC 9:1 to 1:9. (c) Blend AD 9:1 to 1:9. (d) Blend BD 9:1 to 1:9. For each series, feature spacing (■/□) and defect density (◆/◇) as functions of the mass fraction of one component in each blend are plotted. Solid symbols (■/◆) indicate horizontal cylinders as the predominant phase, whereas open symbols (□/◇) indicate a different phase is present. Error bars represent the standard deviation for at least three samples.

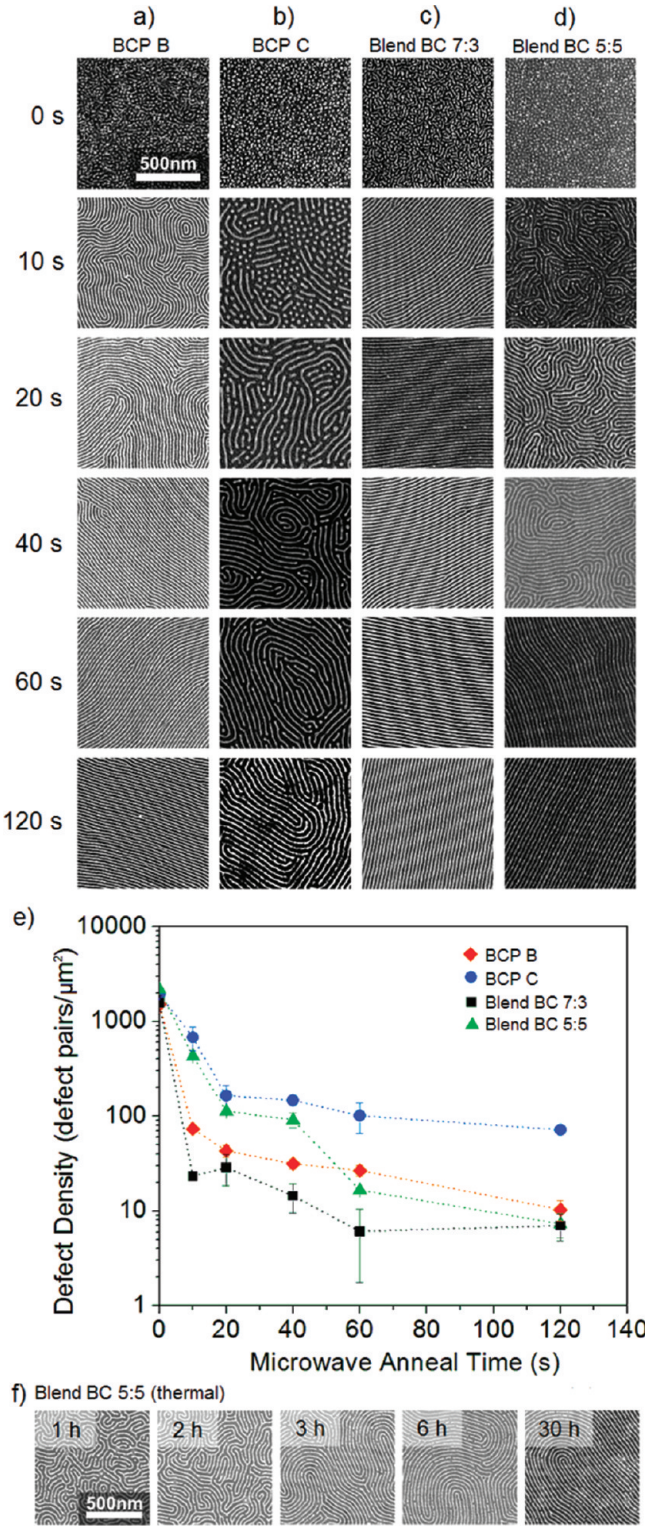

Figure 5. Influence of annealing time over the block copolymer pattern organization for two PS-*b*-P2VP BCPs, B and C, and two BC blends. SEM images of Pt nanostructures templated by microwave annealing of BCPs: (a) BCP B, (b) Blend BC 7:3, (c) Blend BC 5:5, and (d) BCP C. (e) Plots of the evolution of defect density for blends microwave annealed for 0 to 120 s as compared with their constituent block copolymers. Error bars indicate the standard deviation in the measured defect density for at least three separate samples. (f) SEM images of blend BC 5:5 thermally annealed for 1 to 30 h at 200 °C.

blends rather than either of the unmixed components. This furnishes further evidence that ordered, homogeneous patterns may ultimately be achieved in blend films with greater polydispersity, and the result may originate from the smaller BCP functioning as a plasticizer,[47] resulting in more efficient annealing.[48]

The periodicity of linear features is sufficiently sensitive to the composition of each blend to provide good control over a wide range of spacings. With blend AC, for example in Figure 4a, high quality line structures were obtained with blend ratios of 6:4 to 3:7, and in this range, it was possible to vary the line spacings from 26.8 to 30.8 nm. The lowest defect density was observed with a blend ratio of 5:5. With blend BC in Figure 4b, the full range of blend ratios (9:1 to 1:9) led to line structures. Including the neat BCPs on either extreme, a wide range of spacings from 26.4 to 40.9 nm could be formed, and the lowest defect density was observed for blend BC 7:3. Similarly, for blends AD and BD in parts c and d of Figure 4, the lowest defect densities were attained when midrange volume fractions of 5:5 and 7:3 were used, respectively. Using blend AD, linear feature spacings of 32.5 to 38.4 nm were obtained using volume ratios from 6:4 to 4:6, and using blend BD, linear feature spacings from 29.3 to 42.5 nm were obtained with blend ratios from 9:1 to 5:5. Other PS-*b*-P2VP/PS-*b*-P2VP blends also provide the means to control the feature spacing. Examples from blend AB and blend BF are shown in the Supporting Information.

Evolution of Defect Density in Microwave Annealing. To investigate the time evolution of BCP self-assembly, a series of neat and blended BCPs samples were microwave annealed for 10 to 120 s. Parts a−d of Figure 5 show SEM images of platinum nanostructures templated from microwave annealed thin films of BCP B, BCP C, and two blends, BC 7:3 and BC 5:5. The results show that in all cases the morphology is transformed from quasi-hexagonal dot arrays to horizontal cylindrical fingerprint patterns within 10 s, and in the absence of wall-like structures to direct the assembly, low defect densities on the order of 5 to 10 defect pairs·μm^{-2} are attained within 120 s. In contrast, blend BC 5:5 was thermally annealed in vacuum at 200 °C for given times ranging from 1 to 30 h (Figure 5f). Even after 30 h of annealing, the pattern quality has not reached a level comparable to samples microwave annealed for only 2 min.

It is known that larger block copolymers require longer reorganization times;[7] however, blending a relatively small molecular weight BCP (B), with a larger BCP (C), may reduce the reorganization time dramatically, with the smaller block copolymer acting as a plasticizer. Hence the two BC blends shown in Figure 5 organize more quickly, as shown by the lower defect densities at 60 and 120 s, and blend BC 7:3 with the greater fraction of the smaller polymer (B) is expected to reorganize more quickly than blend BC 5:5 with a smaller fraction of B, as is observed.

CONCLUSION

In summary, our study has demonstrated fast ordering of block copolymer nanopatterns in an inexpensive household microwave oven, making the method accessible to any interested researcher. In most cases, highly ordered structures were obtained within 60 s. Binary blends of homologous PS-*b*-P2VP BCPs provide the ability to precisely control the feature spacing with relative ease. Tunable line spacings, ranging from 24.8 to 42.6 nm, were obtained using these binary block copolymer blends. In addition, blending enables assembly into non-native

morphologies inaccessible by each component BCP in its pure form. Combined, the tunability and morphological transformation inherent with blends reduce the need for synthesis of new homologous polymers in order to tune properties via blocks of specified lengths. This approach expands the application of already available polymers and the speed with which they can be self-assembled into ordered, nanoscale structural templates.

■ ASSOCIATED CONTENT

Supporting Information. Details and photos of the wax melting tests, ampule vacuum annealing, the microwave annealing chamber, and the damaged microwave annealing chamber, along with SEM images of platinum nanostructures for PS-*b*-P2VP (32.5k-*b*-12k), blends BF and AB are included. This material is available free of charge via the Internet at http://pubs.acs.org.

■ AUTHOR INFORMATION

Corresponding Author

*E-mail: jburiak@ualberta.ca (J.M.B.); ken.harris@nrc-cnrc.gc.ca (K.D.H).

■ ACKNOWLEDGMENT

This work was supported by NRC-NINT, the University of Alberta, Alberta Innovates Technology Futures, and NSERC. The authors thank the University of Alberta NanoFab for electron beam lithography and clean room support.

■ REFERENCES

(1) *International Technology Roadmap for Semiconductors, 2009 ed.*; Semiconductor Industry Association: San Jose, CA, 2009.
(2) Park, C.; Yoon, J.; Thomas, E. L. *Polymer* **2003**, *44*, 6725–6760.
(3) Darling, S. B. *Prog. Polym. Sci.* **2007**, *32*, 1152–1204.
(4) Black, C. T. *ACS Nano* **2007**, *1*, 147–150.
(5) Black, C. T.; Ruiz, R.; Breyta, G.; Cheng, J. Y.; Colburn, M. E.; Guarini, K. W.; Kim, H.-C.; Zhang, Y. *IBM J. Res. Dev.* **2007**, *51*, 605–633.
(6) Cheng, J. Y.; Ross, C. A.; Smith, H. I.; Thomas, E. L. *Adv. Mater.* **2006**, *18*, 2505–2521.
(7) Bang, J.; Jeong, U.; Ryu, D. Y.; Russell, T. P.; Hawker, C. J. *Adv. Mater.* **2009**, *21*, 4769–4792.
(8) Fasolka, M. J.; Mayes, A. M. *Annu. Rev. Mater. Res.* **2001**, *31*, 323–355.
(9) Hamley, I. W. *Nanotechnology* **2003**, *14*, R39–R54.
(10) Hamley, I. W. *Angew. Chem., Int. Ed.* **2003**, *42*, 1692–1712.
(11) Segalman, R. A. *Mater. Sci. Eng. R Rep.* **2005**, *48*, 191–226.
(12) Ruiz, R.; Dobisz, E.; Albrecht, T. R. *ACS Nano* **2011**, *5*, 79–84.
(13) Guarini, K. W.; Black, C. T.; Zhang, Y.; Babich, I. V.; Sikorski, E. M.; Gignac, L. M. In *Electron Devices Meeting, 2003. IEDM '03 Technical Digest. IEEE International*; IEEE: New York, 2003; pp 22.2.1−22.2.4.
(14) Urbas, A. M.; Maldovan, M.; DeRege, P.; Thomas, E. L. *Adv. Mater.* **2002**, *14*, 1850–1853.
(15) Stoykovich, M. P.; Nealey, P. F. *Mater. Today* **2006**, *9*, 20–29.
(16) Kim, S. O.; Kim, B. H.; Kim, K.; Koo, C. M.; Stoykovich, M. P.; Nealey, P. F.; Solak, H. H. *Macromolecules* **2006**, *39*, 5466–5470.
(17) Kim, H.-C.; Park, S.-M.; Hinsberg, W. D. *Chem. Rev.* **2010**, *110*, 146–177.
(18) Hashimoto, T.; Shibayama, M.; Kawai, H. *Macromolecules* **1983**, *16*, 1093–1101.
(19) Schmidt, K.; Schoberth, H. G.; Ruppel, M.; Zettl, H.; Hansel, H.; Weiss, T. M.; Urban, V.; Krausch, G.; Boker, A. *Nat. Mater.* **2008**, *7*, 142–145.
(20) Stoykovich, M. P.; Müller, M.; Kim, S. O.; Solak, H. H.; Edwards, E. W.; de Pablo, J. J.; Nealey, P. F. *Science* **2005**, *308*, 1442–1446.
(21) Goldacker, T.; Abetz, V.; Stadler, R.; Erukhimovich, I.; Leibler, L. *Nature* **1999**, *398*, 137–139.
(22) Ruzette, A.-V.; Leibler, L. *Nat. Mater.* **2005**, *4*, 19–31.
(23) Tanaka, H.; Hasegawa, H.; Hashimoto, T. *Macromolecules* **1991**, *24*, 240–251.
(24) Stuen, K. O.; Thomas, C. S.; Liu, G.; Ferrier, N.; Nealey, P. F. *Macromolecules* **2009**, *42*, 5139–5145.
(25) Jeong, U.; Kim, H. -C.; Rodriguez, R. L.; Tsai, I. Y.; Stafford, C. M.; Kim, J. K.; Hawker, C. J.; Russell, T. P. *Adv. Mater.* **2002**, *14*, 274–276.
(26) Peng, J.; Gao, X.; Wei, Y.; Wang, H.; Li, B.; Han, Y. *J. Chem. Phys.* **2005**, *122*, 114706.
(27) Jeong, U.; Ryu, D. Y.; Kim, J. K.; Kim, D. H.; Wu, X.; Russell, T. P. *Macromolecules* **2003**, *36*, 10126–10129.
(28) Winey, K. I.; Thomas, E. L.; Fetters, L. J. *Macromolecules* **1991**, *24*, 6182–6188.
(29) Nagpal, U.; Kang, H.; Craig, G. S. W.; Nealey, P. F.; de Pablo, J. J. *ACS Nano* **2011**, *5*, 5673–5682.
(30) Yamaguchi, D.; Hashimoto, T. *Macromolecules* **2001**, *34*, 6495–6505.
(31) Hadziioannou, G.; Skoulios, A. *Macromolecules* **1982**, *15*, 267–271.
(32) Koneripalli, N.; Levicky, R.; Bates, F. S.; Matsen, M. W.; Satija, S. K.; Ankner, J.; Kaiser, H. *Macromolecules* **1998**, *31*, 3498–3508.
(33) Court, F.; Hashimoto, T. *Macromolecules* **2001**, *34*, 2536–2545.
(34) Parnell, A. J.; Pryke, A.; Mykhaylyk, O. O.; Howse, J. R.; Adawi, A. M.; Terrill, N. J.; Fairclough, J. P. A. *Soft Matter* **2011**, *7*, 3721–3725.
(35) Zhang, X.; Harris, K. D.; Wu, N. L. Y.; Murphy, J. N.; Buriak, J. M. *ACS Nano* **2010**, *4*, 7021–7029.
(36) *Handbook of Semiconductor Wafer Cleaning Technology: Science, Technology, and Applications*; Kern, W., Ed.; Noyes Publications: Park Ridge, NJ, 1993.
(37) Chai, J.; Buriak, J. M. *ACS Nano* **2008**, *2*, 489–501.
(38) Chai, J.; Wang, D.; Fan, X.; Buriak, J. M. *Nat. Nanotechnol.* **2007**, *2*, 500–506.
(39) Cheng, J. Y.; Ross, C. A.; Smith, H. I.; Thomas, E. L. *Adv. Mater.* **2006**, *18*, 2505–2521.
(40) Rasband, W. S. *ImageJ*; U. S. National Institutes of Health: Bethesda, MD, 1997.
(41) It should be noted that we expect other non-microwave solvothermal anneal techniques to be capable of annealing BCPs in a comparable manner, provided the method is compatible with high pressure solvents and that substrate heating is rapid; however, attempts to emulate this have faced practical limitations.[35]
(42) Bates, F. S.; Fredrickson, G. H. *Phys. Today* **1999**, *52*, 32–38.
(43) Lynd, N. A.; Meuler, A. J.; Hillmyer, M. A. *Prog. Polym. Sci.* **2008**, *33*, 875–893.
(44) Matsushita, Y.; Noro, A.; Iinuma, M.; Suzuki, J.; Ohtani, H.; Takano, A. *Macromolecules* **2003**, *36*, 8074–8077.
(45) Noro, A.; Cho, D.; Takano, A.; Matsushita, Y. *Macromolecules* **2005**, *38*, 4371–4376.
(46) Kléman, M. *Points, lines, and walls: in liquid crystals, magnetic systems, and various ordered media*; J. Wiley: Chichester, U.K., and New York, 1983.
(47) Shin, D. O.; Jeong, J.-R.; Han, T. H.; Koo, C. M.; Park, H.-J.; Lim, Y. T.; Kim, S. O. *J. Mater. Chem.* **2010**, *20*, 7241–7247.
(48) For instance, it can be calculated from the available polymer data (Table 1) that blend AD 5:5 has an overall polydispersity of 2.36, the largest in the entire series and larger than either component polymer, yet of the series it possesses a low defect density after 60 s annealing, indicating that high polydispersity is not a significant factor affecting ordering of nanostructures for homologous BCPs.